

Case Report

## Spontaneous adenocarcinoma with giant cell formation in the accessory sex glands in a male Sprague-Dawley rat

Shingo Miyazaki\*, Takashi Ogawa<sup>1</sup>, Tomoya Onozato<sup>1</sup>, Yuji Okuhara<sup>1</sup>, Tatsuya Nagasawa<sup>1</sup>, and Morimichi Hayashi<sup>1</sup>

<sup>1</sup> Safety Research Laboratory, Kissei Pharmaceutical Co., Ltd., 2320-1 Maki, Hotaka, Azumino, Nagano 399-8305, Japan

**Abstract:** In this study, we report the features of an adenocarcinoma with giant cell formation spontaneously occurring in the accessory sex glands of a male 10-month-old Sprague-Dawley rat. A milky white mass was found in the region corresponding to the left seminal vesicle and the left coagulating gland. Histologically, tumor cells exhibited diverse growth patterns, including glandular/trabecular, cystic, and sheet-like growth areas. The tumor cells were pleomorphic, with round- or oval-shaped nuclei and abundant eosinophilic cytoplasm. Mitotic figures were occasionally observed. Giant cells were also prominent in the sheet-like growth area, with intracytoplasmic vacuoles containing eosinophilic material. The stroma was rich in collagen fibers and fibroblasts. Numerous inflammatory cells were observed in the glandular and cystic lumina and stroma. Immunohistochemically, the tumor cells were positive for cytokeratin AE1/AE3 and proliferating cell nuclear antigen. In the sheet-like growth area, some of the tumor cells and giant cells were positive for vimentin in the cytoplasm adjacent to the nucleus. Electron microscopy revealed that the tumor cells contained a small number of mitochondria and rough endoplasmic reticulum, and had no basement membrane or desmosome. The giant cells occasionally contained variably sized intracytoplasmic lumina and globular filamentous bodies, probably corresponding to vimentin. Considering these morphological features, the tumor was diagnosed as an adenocarcinoma with the formation of giant tumor cells originating from the male accessory sex glands. (DOI: 10.1293/tox.2021-0019; J Toxicol Pathol 2021; 34: 345–351)

**Keywords:** Sprague-Dawley rats, male accessory sex glands, adenocarcinoma, spontaneous, giant cells

There are many reports on the incidence of spontaneous tumors in Sprague-Dawley (SD) rats. However, malignant male accessory sex gland tumors, including adenocarcinoma, squamous cell carcinoma, carcinosarcoma, malignant neuroendocrine tumor, and malignant granular cell tumor, have a very low incidence<sup>1–3</sup>, with only a few existing reports. The previous studies demonstrated that adenocarcinoma in the male accessory gland had a cribriform, comedo-type, papillary glandular/tubular, or solid growth pattern<sup>1, 4, 5</sup>. In those cases, many tumor cells showed an epithelial growth pattern, such as glandular/trabecular or cystic, but some tumor cells showed a sheet-like growth pattern with giant cell formation, which had not been described in previous reports. Herein, we report the histological, immunohistochemical, and ultrastructural features of an adenocarcinoma spontaneously occurring in the accessory sex glands of a male SD rat.

A Male Crl:CD(SD) rat aged 9 months was purchased from Charles River Laboratories Japan, Inc. (Yokohama, Japan). The rat was used in a 4-week repeated-dose study aimed at investigating the pharmacological effects of a pharmaceutical compound assigned to the low-dose group. No significant changes in clinical signs or body weight were observed during the treatment period. The animal was euthanized and necropsied at 10 months of age after the completion of the study. At necropsy, an intraperitoneal mass of 2.5 × 1.5 × 1.5 cm size and milky-white color was found in the region corresponding to the left seminal vesicle and left coagulating gland. The mass was poorly demarcated from the surrounding tissue (Fig. 1). The left seminal vesicle, left coagulating gland, and dorsal prostate were not clearly visible, although the right seminal vesicle with coagulating gland and ventral prostate with normal appearance were present outside the mass. The cut surface of the mass appeared milky-white with pus or necrotic areas. No other gross lesions were observed in any of the organs. The animal experiment complied with the Guide for Care and Use of Experimental Animals of the Safety Research Laboratory, Kissei Pharmaceutical Co., Ltd.

The mass was fixed in 10% phosphate-buffered formalin, embedded in paraffin, cut into 3 μm sections, and stained with hematoxylin-eosin (HE) for microscopic examination. Additional histochemical stains, including periodic acid-Schiff (PAS) and Masson's trichrome (MT), were

Received: 19 March 2021, Accepted: 30 June 2021

Published online in J-STAGE: 23 July 2021

\*Corresponding author: S Miyazaki

(e-mail: shingo\_miyazaki@pharm.kissei.co.jp)

©2021 The Japanese Society of Toxicologic Pathology

This is an open-access article distributed under the terms of the Creative Commons Attribution Non-Commercial No Derivatives

(by-nc-nd) License. (CC-BY-NC-ND 4.0: <https://creativecommons.org/licenses/by-nc-nd/4.0/>).



also used. Immunohistochemical staining was performed with an EnVision™ + Dual Link System-HRP kit (Dako A/S, Glostrup, Denmark) and antibodies against cytokeratin AE1/AE3, vimentin, S100, desmin, mesothelin, neurofilament, Iba-1, and proliferating cell nuclear antigen (PCNA). The sources and clones of these antibodies and the results of the immunohistochemical staining are shown in Table 1. For electron microscopic examination, pieces of formalin-fixed tissue were immersed in a half-strength Karnovsky solution and fixed in 1% osmium tetroxide. Ultrathin sections were stained with uranyl acetate and lead citrate, evaporated

with carbon, and then observed under a transmission electron microscope (JEM-1200EX; JEOL Ltd., Tokyo, Japan).

Histologically, the tumor without a capsule was adjacent to the seminal vesicle, coagulation gland, and ureter (Fig. 2). The boundary between the tumor and surrounding tissue was unclear, and a part of the coagulation gland was involved at the periphery of the tumor. In addition, a large abscess and necrosis were present in the central part of the tumor. Most of the tumor mass was occupied by fibrous stroma, in which epithelial-like tumor cells with variable growth patterns were scattered and proliferated. The

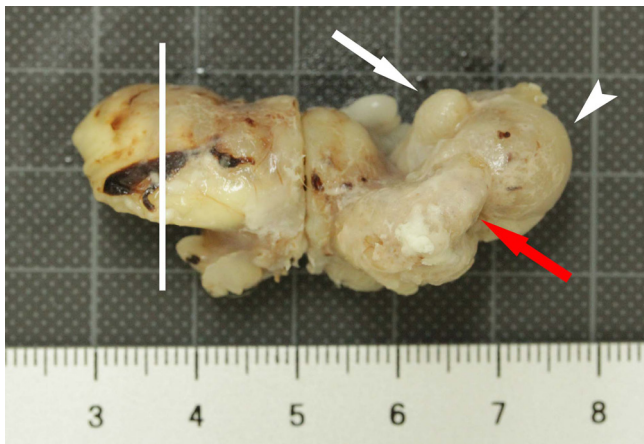


**Fig. 1.** Gross appearance of the formalin-fixed milky white mass from a male SD rat. The mass was located in the region corresponding to the left seminal vesicle and left coagulating gland. The white arrow, arrowhead, and red arrow indicate the urinary bladder, ventral prostate, and right seminal vesicle, respectively. The vertical line indicates a cross section of Fig. 2.

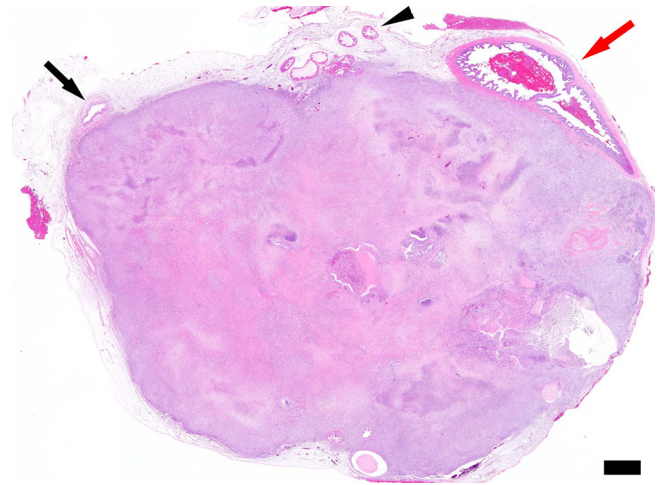


**Fig. 2.** Loupe image of the tumor. The tumor was adjacent to the ureter (black arrow), coagulation gland (arrow-head), and seminal vesicle (red arrow). A large abscess and necrosis were present in the central part of the tumor. HE staining. Bar=1 mm.

**Table 1.** Antibodies Used in Immunohistochemistry and Results of Immunohistochemical Staining

Antibody	Manufacturer	Host species	Clonality (clone name)	Dilution ratio	Antigen activation treatment method (solution)	Results		
						Tumor cells	Giant cells	Stromal fibroblast-like spindle cells
Cytokeratin	Dako	Mouse	Monoclonal (AE1/AE3)	1:5	Microwave, 12 min (Dako Target retrieval Solution)	+++	+++	-
Desmin	Thermo Fisher Scientific	Rabbit	Polyclonal	1:200		-	-	+
Iba-1	Bioss Inc.	Rabbit	Polyclonal	1:2,000	Protease XXV, 10 min, room temperature	-	-	-
Mesothelin	Immuno-Biological Laboratories	Rabbit	Polyclonal	1:2,000		-	-	-
Neurofilament	Dako	Mouse	Monoclonal (2F11)	1:500		-	-	-
PCNA	Dako	Mouse	Monoclonal (PC10)	1:800	Microwave, 12 min (Dako Target retrieval Solution)	+++	+++	+
S100	Dako	Rabbit	Polyclonal	1:5	Microwave, 12 min (Dako Target retrieval Solution)	-	-	-
Vimentin	Dako	Mouse	Monoclonal (V9)	1:1		+ (sheet-like growth area only)	+	+++

Immunohistochemical staining intensity: negative (-), slightly positive (+), and strongly positive (+++).



growth patterns of the tumor cells were glandular/trabecular (Fig. 3a), cystic (Fig. 3b), and sheet-like (Fig. 3c). The tumor cells were pleomorphic, with round- or oval-shaped nuclei exhibiting marked anisokaryosis and containing one or two distinct nucleoli. Mitotic figures were occasionally observed. The tumor cell cytoplasm was abundant and eosinophilic. Abundant fibrous connective tissue and fibroblast-like spindle cells were found in the stroma. In the glandular/trabecular growth area, which was the most frequent growth pattern in the tumor, some tumor cells underwent transformation to a spindle-shaped phenotype. Numerous giant cells were observed in the sheet-like growth areas (Fig. 3d). Giant cells with one or two large atypical nuclei and variably sized cytoplasmic vacuoles containing weakly eosinophilic and PAS-positive materials were scattered singly or in small clusters among collagen fibers. A pronounced infiltration of neutrophils, eosinophils, and macrophages was observed in the glandular and cystic lumina and stroma throughout the entire tumor mass.

MT staining revealed abundant collagen fibers in the stroma (Fig. 4a). Immunohistochemically, the tumor cells, including giant cells, were positive for cytokeratin AE1/

AE3 in all growth areas of the tumor (Fig. 4b), and many were also positive for PCNA (Fig. 4c) within the entire tumor mass. The stromal fibroblast-like spindle cells were strongly positive for vimentin expression (Fig. 4d), but the tumor cells that transformed to spindle-shaped cells were negative. In the sheet-like growth area, some of the tumor cells and giant cells also showed a positive reaction for vimentin in the cytoplasm adjacent to the nucleus (Fig. 4e). A few spindle-shaped cells in the stroma were positive for desmin. No positive reaction for S100, neurofilament, Iba-1, or mesothelin was observed in any growth area.

Electron microscopy revealed that the cytoplasmic organelles of the tumor cells in the sheet-like growth area were relatively scant and consisted of a small number of mitochondria and rough endoplasmic reticulum (Fig. 5a and 5b). No basement membranes or desmosomes were observed. A few secretory granules were found only on the luminal side of the tumor cells in the cystic growth area. The giant cells in the sheet-like growth area contained variably sized intracytoplasmic lumina with well-developed microvilli on their inner surface (Fig. 5c and 5d), and aggregated intermediate filaments involving many mitochondria adjacent to

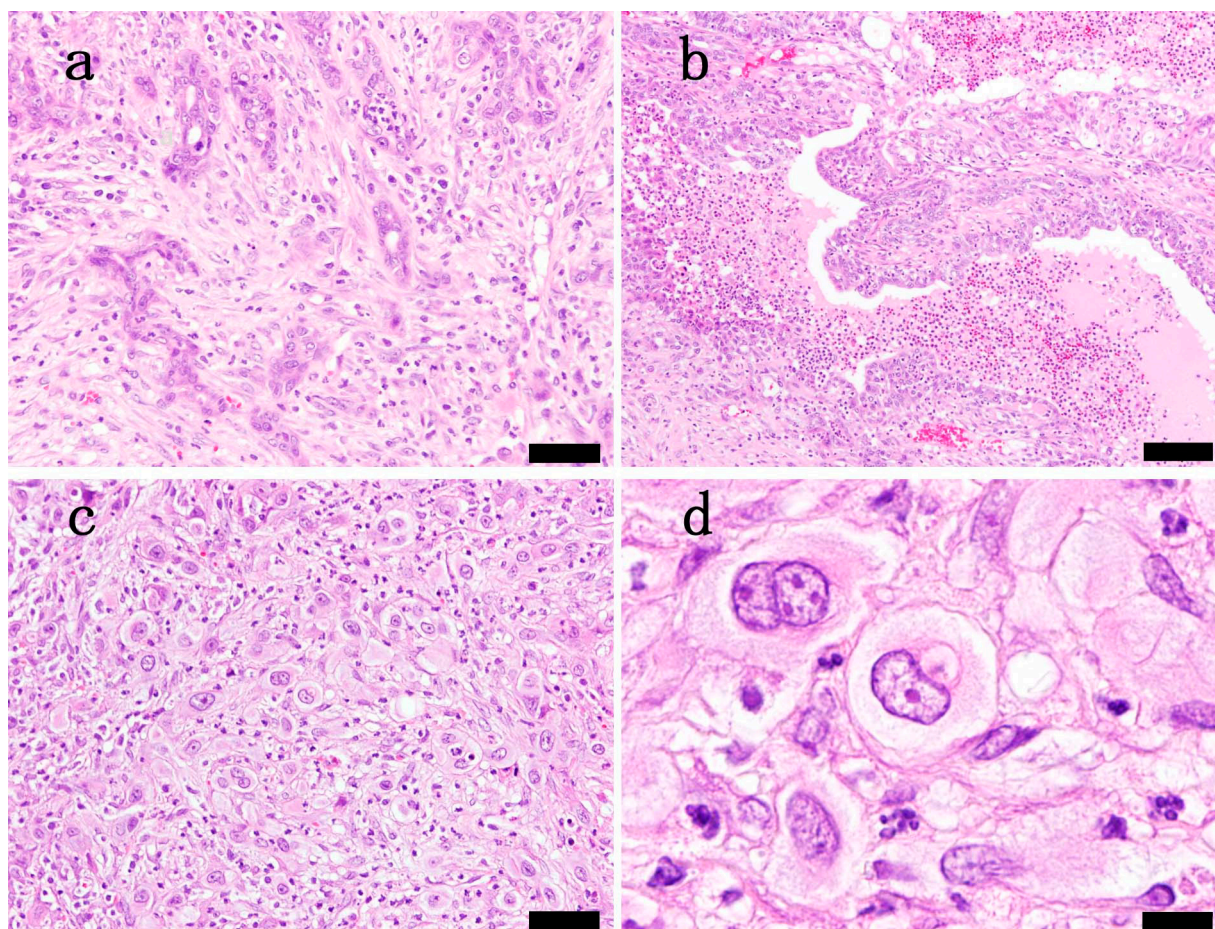


**Fig. 3.** Histological appearance of different growth patterns in the tumor. a) Glandular/trabecular growth area. b) Cystic growth area. c) Sheet-like growth area. d) Giant cells with intracytoplasmic vacuoles in the sheet-like growth area. HE staining. Bars=50  $\mu$ m (a and c), 100  $\mu$ m (b), and 10  $\mu$ m (d).



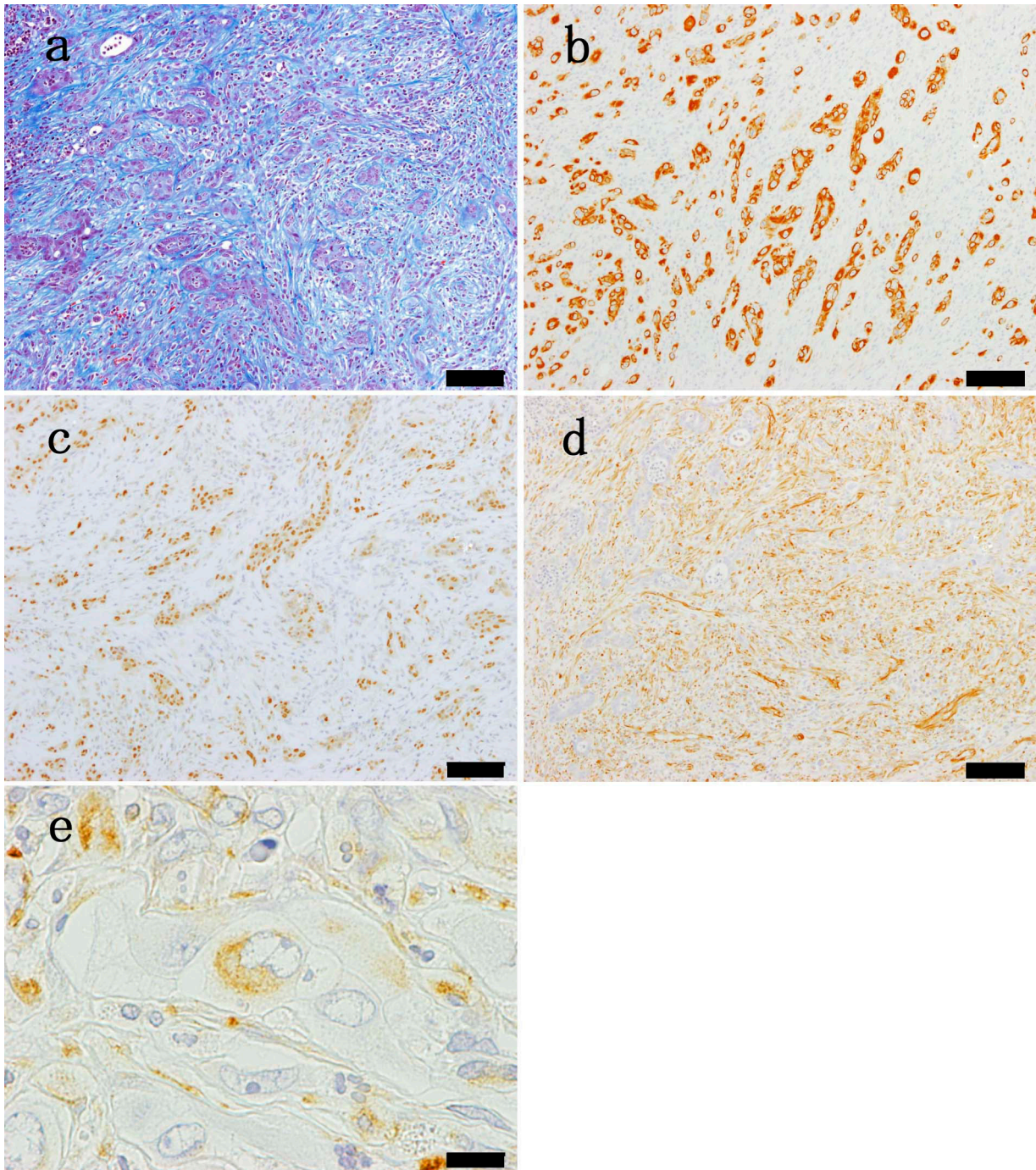


**Fig. 4.** a) MT staining showed abundant collagen fibers in the stroma. b and c) Tumor cells were positive for cytokeratin AE1/AE3 and PCNA, respectively. d) Stromal spindle-shaped cells were positive for vimentin. e) Some tumor cells and giant cells were also positive for vimentin in the cytoplasm adjacent to the nucleus (e). Bars=100  $\mu$ m (a, b, c and d) and 10  $\mu$ m (e).

the nucleus. These features are termed globular filamentous bodies<sup>6</sup> (Fig. 5e and 5f), and are probably consistent with vimentin-positive immunohistochemical staining.

In the present case, the tumor mass was found in the region corresponding to the left seminal vesicle and left coagulation gland of a male 10-month-old SD rat that was assigned to the low-dose group in a 4-week repeated-dose study of a pharmaceutical compound. No proliferative le-

sions were noted in any other animals in this study; therefore, the onset of this lesion was considered spontaneous. Numerous inflammatory cells and abundant stromal connective tissue were observed throughout the tumor mass. Although the marked inflammatory cell infiltration raises the possibility that this proliferative lesion may have been a reactive hyperplasia of glandular epithelial cells caused by inflammation, we concluded that it was a neoplastic le-



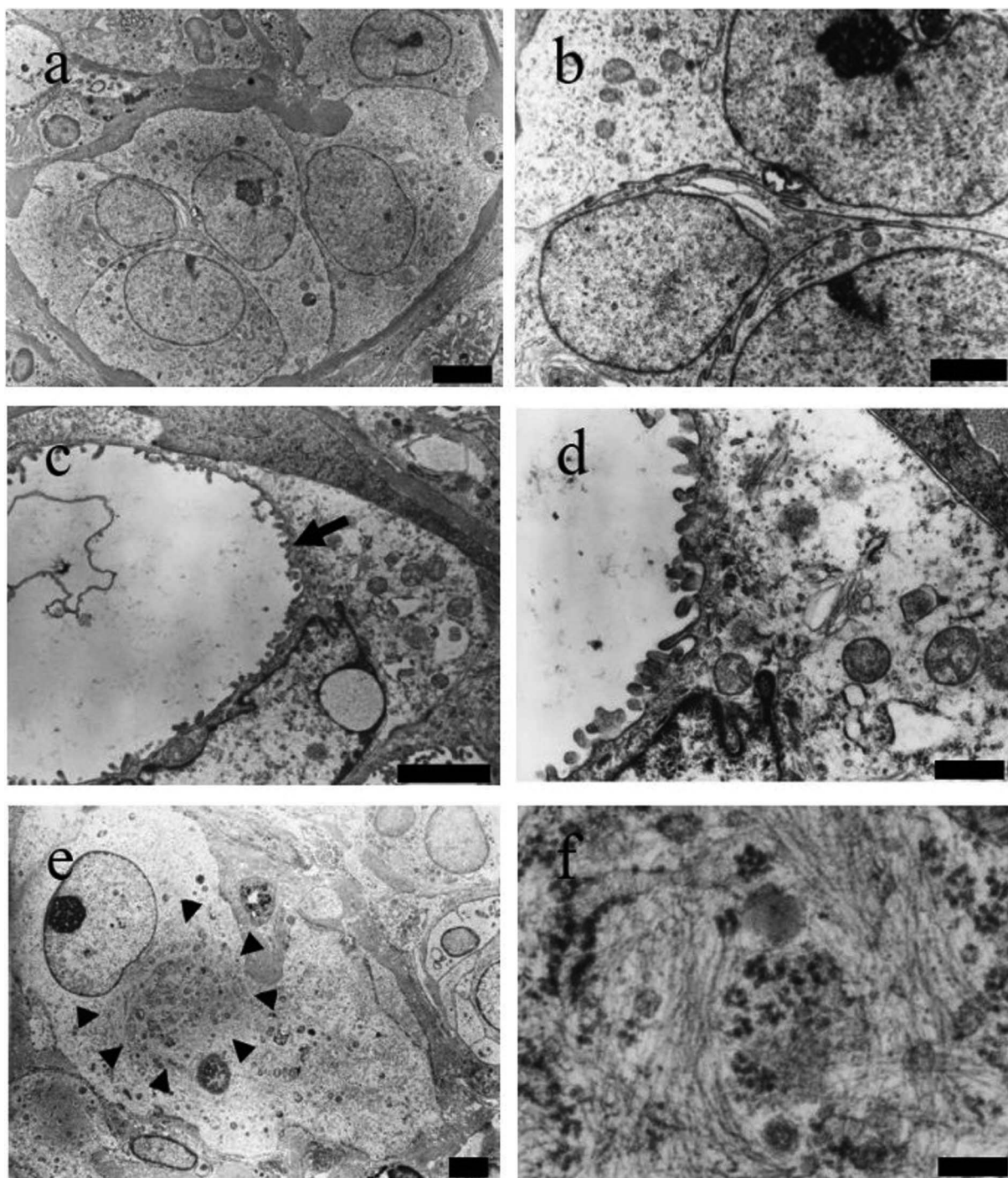


**Fig. 5.** Ultrastructural appearance of tumor cells and giant cells in the sheet-like growth area. a and b) Tumor cells with a small number of mitochondria and rough endoplasmic reticulum. c) Giant cells with intracytoplasmic lumina lined by microvilli (arrow). d) High magnification of the intracytoplasmic lumina. e) Giant cells with globular filamentous bodies adjacent to the nucleus (arrowheads). f) High magnification of the globular filamentous bodies. Bars=5  $\mu$ m (a), 2  $\mu$ m (b, c and e), 500 nm (d), and 100 nm (f).

sion because the proliferative cells had a markedly atypical morphology. This morphology included various growth patterns, giant cell formation, and transformation to spindle-shaped cells.

Most of the tumor cells, including giant cells, showed an epithelial growth pattern and immunohistochemically

positive staining for cytokeratin AE1/AE3, suggesting that they originated from epithelial cells or mesothelial cells. Considering that the tumor mass involved the seminal vesicle and coagulating gland, an adenocarcinoma originating from glandular epithelial cells of the accessory sex glands is the most likely diagnosis. Differential diagnoses include

urothelial cell carcinoma and malignant mesothelioma. Urothelial cell carcinoma was not applicable to this tumor because there was no papillary or solid growth pattern of urothelial cells<sup>7</sup>, and no evidence of continuity to the urinary tract. A diagnosis of malignant mesothelioma was also not applicable to this tumor since fronds or papillary structures characteristic of that tumor type were not observed<sup>8</sup>, and the tumor cells were negative for mesothelin, a mesothelial cell marker<sup>9, 10</sup>. Furthermore, carcinosarcoma characterized by a mixture of pleomorphic epithelial tumor cells and spindle tumor cells<sup>1</sup> could also be considered as a differential diagnosis. However, most of the spindle-shaped cells in the tumor mass were non-neoplastic fibroblasts, and the presence of spindle tumor cells was not prominent, indicating that a diagnosis of carcinosarcoma was not applicable to this tumor.

Spontaneous neoplasms of the male accessory sex glands are uncommon in most rat and mouse strains, including SD rats<sup>1-4, 11, 12</sup>. Some strains, notably ACI/segHapBR rats, have a high incidence of naturally occurring prostate carcinoma<sup>13</sup>. Various carcinogens have also been reported to induce adenocarcinomas of male accessory sex glands in rodents<sup>14, 15</sup>. In both spontaneously occurring and carcinogen-induced cases, the tumor cells often display a pleomorphic appearance and a diverse growth pattern, and there is also often an association with inflammation and fibrosis<sup>1, 5, 16</sup>. When the tumor is large and invasive into other accessory glands, it is difficult or impossible to precisely determine the glands of origin<sup>1, 5, 16</sup>. All the above-mentioned histological features are consistent with our results.

Prominent giant cell formation was a characteristic of the present case. Giant cell formation is often seen in undifferentiated and anaplastic tumors, and tumor giant cells possess only a single huge polymorphic nucleus or two or more large hyperchromatic nuclei<sup>17</sup>. These histological features are similar to those observed in the present case. Another condition possibly leading to giant cell formation is an inflammatory response, such as Langhans or foreign body giant cells derived from macrophages<sup>18</sup>. However, the giant cells in the present case were not considered inflammatory giant cell macrophages due to a negative reaction for Iba-1. These results indicate that this tumor was characterized by marked anaplasia with giant tumor cell formation.

In conclusion, we report a case of spontaneous adenocarcinoma with formation of giant tumor cells in the male accessory sex glands in a SD rat, although it is impossible to determine the exact site of origin. The results of our research suggest that adenocarcinomas of the male accessory sex glands in rats may present a pleomorphic appearance and a diverse growth pattern, regardless of the rat strain or pathogenesis (spontaneous or carcinogen-induced).

**Disclosure of Potential Conflicts of Interest:** The authors declare that they have no conflicts of interest.

**Acknowledgments:** We are grateful to Yoshimi Tsukahara, Rie Nakano, and Sayuri Yamagishi for their excellent technical assistance.

## References

1. Creasy D, Bube A, de Rijk E, Kandori H, Kuwahara M, Masson R, Nolte T, Reams R, Regan K, Rehm S, Rogerson P, and Whitney K. Proliferative and nonproliferative lesions of the rat and mouse male reproductive system. *Toxicol Pathol.* **40**(Suppl): 40S–121S. 2012. [Medline] [CrossRef]
2. Giknis MLA, and Clifford CB. Compilation of spontaneous neoplastic lesions and survival in CrI:CD (SD) rats from control groups. 2004, from Charles River Laboratories website: [https://www.criver.com/sites/default/files/Technical%20Resources/Compilation%20of%20Spontaneous%20Neoplastic%20Lesions%20and%20Survival%20in%20CrI-CD\\_SD\\_%20Rats%20from%20Control%20Group%20-%20March%202004.pdf](https://www.criver.com/sites/default/files/Technical%20Resources/Compilation%20of%20Spontaneous%20Neoplastic%20Lesions%20and%20Survival%20in%20CrI-CD_SD_%20Rats%20from%20Control%20Group%20-%20March%202004.pdf)
3. Chandra M, Riley MG, and Johnson DE. Spontaneous neoplasms in aged Sprague-Dawley rats. *Arch Toxicol.* **66**: 496–502. 1992. [Medline] [CrossRef]
4. Shoda T, Mitsumori K, Imazawa T, Toyoda K, Tamura T, Takada K, and Takahashi M. A spontaneous seminal vesicle adenocarcinoma in an aged F344 rat. *Toxicol Pathol.* **26**: 448–451. 1998. [Medline] [CrossRef]
5. Jones TC, Morhr U, and Hunt RD, editors. *Monographs on Pathology of Laboratory Animals, Genitalsystem.* Springer-Verlag, New York. 252–286. 1987.
6. Ghadially FN. *Ultrastructural pathology of the cell and matrix*, 3rd ed. Butterworths, London. 906–911. 1988.
7. Frazier KS, Seely JC, Hard GC, Betton G, Burnett R, Nakatsuji S, Nishikawa A, Durchfeld-Meyer B, and Bube A. Proliferative and nonproliferative lesions of the rat and mouse urinary system. *Toxicol Pathol.* **40**(Suppl): 14S–86S. 2012. [Medline] [CrossRef]
8. Greaves P, Chouinard L, Ernst H, Mecklenburg L, Prui-boom-Brees IM, Rinke M, Rittinghausen S, Thibault S, Von Erichsen J, and Yoshida T. Proliferative and non-proliferative lesions of the rat and mouse soft tissue, skeletal muscle and mesothelium. *J Toxicol Pathol.* **26**(Suppl): 1S–26S. 2013. [Medline] [CrossRef]
9. Doi T, Kotani Y, Takahashi K, Hashimoto S, Yamada N, Kokoshima H, Tomonari Y, Wako Y, and Tsuchitani M. Malignant mesothelioma in the thoracic cavity of a Crj:CD(SD) rat characterized by round hyalinous stroma. *J Toxicol Pathol.* **23**: 103–106. 2010. [Medline] [CrossRef]
10. Ohnuma-Koyama A, Yoshida T, Takahashi N, Akema S, Takeuchi-Kashimoto Y, Kuwahara M, Nagaike M, Inui K, Nakashima N, and Harada T. Malignant peritoneal mesothelioma with a sarcomatoid growth pattern and signet-ring-like structure in a female f344 rat. *J Toxicol Pathol.* **26**: 197–201. 2013. [Medline] [CrossRef]
11. Giknis MLA, and Clifford CB. Neoplastic and non-neoplastic lesions in the Charles River Wistar Hannover [CRL:WI (Han)] rat. 2011, from Charles River Laboratories website: <https://animalab.hu/download/903c98ad-7a53-4371-a72a-0728737b0670/neoplastic-and-non-neoplastic-lesions-in-the-charles-river-wistar-hannover-crl-wihan-rat>

march-2011.pdf

12. Haseman JK, Hailey JR, and Morris RW. Spontaneous neoplasm incidences in Fischer 344 rats and B6C3F1 mice in two-year carcinogenicity studies: a National Toxicology Program update. *Toxicol Pathol.* **26**: 428–441. 1998. [[Medline](#)] [[CrossRef](#)]
13. Ward JM, Reznik G, Stinson SF, Lattuada CP, Longfellow DG, and Cameron TP. Histogenesis and morphology of naturally occurring prostatic carcinoma in the ACI/segHapBR rat. *Lab Invest.* **43**: 517–522. 1980. [[Medline](#)]
14. Pour PM. A new prostatic cancer model: systemic induction of prostatic cancer in rats by a nitrosamine. *Cancer Lett.* **13**: 303–308. 1981. [[Medline](#)] [[CrossRef](#)]
15. Pour PM. Prostatic cancer induced in MRC rats by N-nitrosobis(2-oxopropyl)-amine and N-nitrosobis(2-hydroxypropyl)amine. *Carcinogenesis.* **4**: 49–55. 1983. [[Medline](#)] [[CrossRef](#)]
16. Bosland MC, Tuomari DL, Elwell MR, Shirai T, Ward JM, and McConnell RF. Proliferative lesions of the prostate and other accessory sex glands in male rats, URG-4. In: *Guides for Toxicologic Pathology*. STP/ARP/AFIP, Washington DC. 4–20. 1998.
17. Kumar V, Abbas AK, Aster J, eds. *Robbins and Cotran pathologic basis of disease*, 9th ed, professional ed. Elsevier Saunders, Canada. 267–275. 2014.
18. Mariano M, and Spector WG. The formation and properties of macrophage polykaryons (inflammatory giant cells). *J Pathol.* **113**: 1–19. 1974. [[Medline](#)] [[CrossRef](#)]